Experimental Studies of Terrestrial
mm-Wave Links—A Review
Part 1: Attenuation Due to Atmospheric Particles

Adel Ali, Mohamed Hassan and Mohammed Alhaider

Electrical Engineering Department, King Saud University,
Riyadh, Saudi Arabia

Recent experimental studies on terrestrial mm-wave links are reviewed in this paper. In Part 1, attenuation by atmospheric hydrometeors including fog, clouds, snow and rain is presented with more emphasis on rain. Effects of sand and dust storms are discussed through the few experimental systems reported in the literature. Each section starts by an explanation of the physical phenomenon followed by a summary of the major, recent experiments with emphasis on experimental set up and main results. Clear air phenomena, diversity and data processing are dealt with in Part 2. Modelling, theoretical studies and slant paths are outside the scope of this review.

Introduction

The utilization of frequency bands above 10 GHz for line of sight communications has attracted increasing attention during the last two decades due to the ever growing demand for new services and the crowding of lower frequency bands. However, practical applications in communication have so far been few. There are two main reasons for this; (i) until recently, the development of reliable components has been slow and (ii) atmospheric attenuation may degrade the operation of any free-space link system. Recent progress in component development coupled with the congestion present at lower frequencies has revived interest in the millimetric waveband. Many experimental and theoretical studies have been reported in the last few years, giving a better understanding of various propagation phenomena and suggesting possible systems layouts. Unfortunately, no 'cook book' method is available for millimetric link design, since results obtained for a climate region of one climate are not directly

applicable to other regions of different climates. Further studies are still needed to answer many questions regarding the maximum possible hop length, channel bandwidth, types of digital modulation and diversity.

The aim of this paper is to present a survey of experimental terrestrial mm-link systems and to outline the areas of needed studies. Although several reviews have been reported [1-10], they were either general, or dealt with specific phenomena.

The present review should be useful to engineers and researchers planning an experimental link system at the mm-band. Section 2 surveys the main experimental studies of free-space attenuation and power loss due to hydrometeors and other particles. Scintillation fading is also described. In Section 3 an outline of Part 2 of this paper is given.

Measured Parameters

In the millimetric wave band, the signal is affected by several natural mechanisms causing signal reductions relative to a free space level. These are summarized in Fig. 1.

Free Space Attenuation

In the electromagnetic spectrum, millimetric wave frequencies occupy a decade frequency range from about 30 GHz to 300 GHz. The troposphere affects the propa-
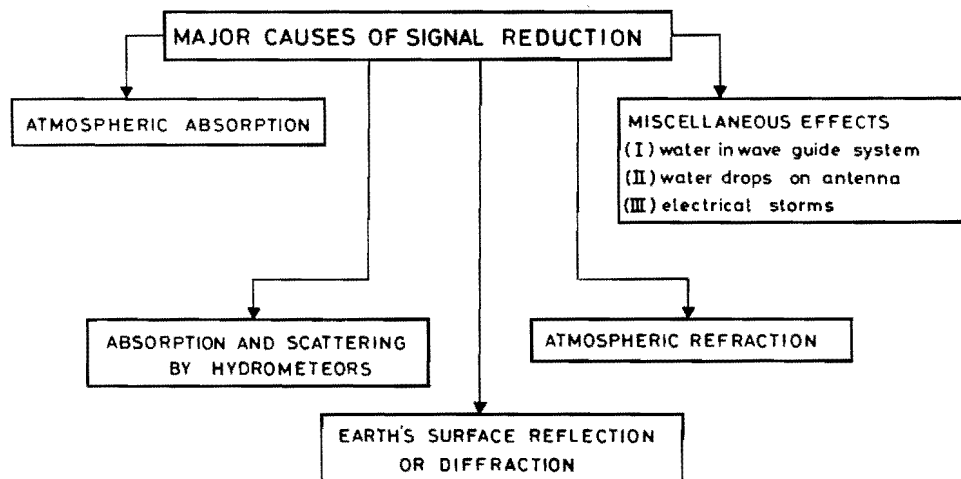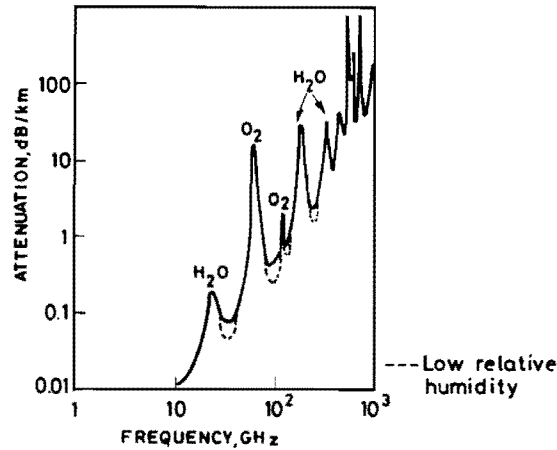

Fig. 1

Fig. 2: Attenuation Due to Gaseous Constituents

gation of millimeter-waves as it does at other frequencies, but with some differences. This propagation is affected by the tropospheric absorption, caused by the interaction between electromagnetic waves and gases, such as molecular oxygen and water vapour.

Figure 2 gives the specific attenuation due to gaseous constituents as a function of frequency for standard atmospheric conditions [11-14]. The frequency spans in the vicinity of attenuation minima are called 'windows'. Windows are at 25-50 GHz, 70-110 GHz, 130-160 GHz, and 200-280 GHz. These are usually taken as the operating regions, and are extremely wide compared with available microwave bandwidths.

Theory verified by field measurement shows that attenuation is increased with increasing humidity (see Fig. 2), and this increase is highly variable and depends on water vapour clusters and the visible liquid water droplets [11]. Daily analysis of molecular absorption is not needed as its variations are not so large compared with other meteorological effects.

Attenuation by Atmospheric Hydrometeors

Hydrometeors are defined as condensation of water vapour which is suspended or falls in the atmosphere. They can be in the solid form, like snow or ice crystal; in the liquid form, like rain or fog; or in the mixed form, like wet snow or melting hail. These hydrometeors extract energy from the passing radio wave and scatter this energy into directions away from the receiving antenna. Some of this energy is also absorbed by the particulates.

Absorption and scattering by hydrometeors constitute one of the main limitations in millimetric wave propagation. Theoretical approaches for estimating the influence of such hydrometeors are available. However, information–on the actual and the expected size distribution and sometimes about the shape along the propagation path–is lacking. This makes measurements necessary and experimental studies very desirable. Some of these measurements are summarized below.

Attenuation due to Fog. The liquid water content in heavy fog is lower than that of heavy rain. Therefore, fog attenuates microwaves much less than does rain [15], but in submillimetric band the reverse is true, as shown in Fig. 3.

Weibel and Dressel [16] set up a 2 km millimetric wave link operating at 90.5 GHz at Bayside, N.Y.; not only to measure fog attenuation but also to supply data on atmospheric millimeter-wave propagation. The transmission path was mainly over water.

During measurements, the average optical visibility was noted as an assumed measure of the water content of each fog. They obtained slightly higher loss than that calculated by Ryde and Ryde [17] under conditions of light fog.

Attenuation by fog in $dB/km/g/m^3 = -1.347 + 0.0372 + (18.0/\lambda) - 0.022\,T$, where λ is the wavelength in mm and T is the temperature in °C, 3 mm $< \lambda <$ 30 mm; $-8\,°C < T < 25\,°C$. If fog density data M is not available but visibility V is available, then the relation $M = (0.024/V)^{1.54}$ may be used.

Ho *et al.* [18] established two links, operating at 110 GHz and 36 GHz, along a common 4.1 km path across central London, half over a park and the rest over buildings. They found that maximum fog attenuation was more than 0.5 dB for the 36 GHz signal and more than 3 dB for the 110 GHz signal. The visibility during that period was of the order of 300 m.
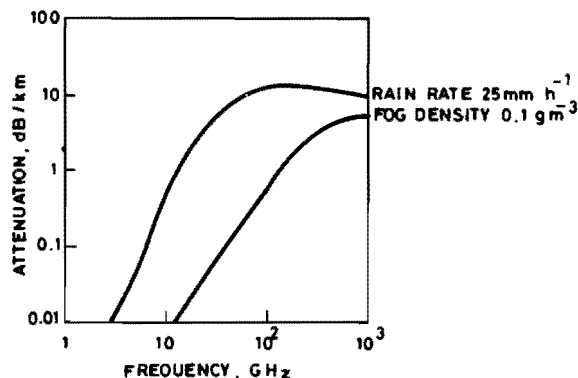

Fig. 3:   Attenuation of Water in Various Forms

Attenuation due to Clouds. Attenuation by clouds is significant and must be taken into consideration in earth-space communication system planning. As we are not dealing with earth-space experimental links here, measurements carried out for cloud attenuation will not be considered.

Attenuation due to Snow. Few reports of excessive attenuation due to snow are found in the literature [16, 19], though it is known that melting snow is heavily attenuating. Dry snow causes little attenuation in the frequency range 10–40 GHz. Losses due to snow on antenna reflectors is found to be less than that due to water on the reflectors during rainfall. However, accumulated snow on a reflector may cause reflection losses of 10–20 dB.

Attenuation due to Rain. Rain is one of the most important factors affecting the propagation of radio waves in the millimetric waveband. A heavy rainstorm may cause severe attenuation, as high as 20 dB/km, at a frequency of 55 GHz and increase as the frequency increases (Fig. 4). Therefore, it is very desirable for the communications engineer to be aware of the problems of attenuation before establishing a mm-communication link.

Considerable attention has been given to the problem of rain induced attenuation by many researchers. They made field studies, followed theoretical prediction methods and used simulation techniques. They employed direct and indirect methods of measurements, and conducted experiments on terrestrial systems as well as on earth-space systems.

In this section we shall emphasize the different experimental terrestrial links used in measuring attenuation caused by rain.
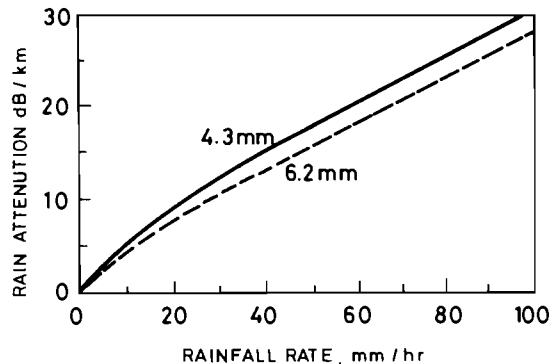

Fig. 4:   Rain Attenuation vs. Rainfall Rate

A 4.1 km communication link, installed across central London and operated at 36 GHz and 110 GHz, was described previously [18]. The authors computed the ratio of the attenuations measured simultaneously at the two frequencies, for about 20 hours of widespread rainfall. They plotted this ratio as a function of the attenuation at 110 GHz. This ratio curve was found to fit the ratio curve computed using the Laws–Parsons drop size distribution.

Therefore, they concluded that the rainfall attenuation at a given mm-wavelength can be computed from a knowledge of the attenuation at another wavelength, and the use of the Laws–Parsons raindrop size distribution. This eliminates the necessity of knowing the rainfall rate to determine attenuation at another frequency given a knowledge of the measured attenuation at the reference frequency.

Weibel and Dressel [16] set up an experimental 3.32 mm (90.5 GHz) link at Bayside, N.Y. as described in Section 2.2.1. They measured the attenuation against rainfall rate and showed that a range of attenuation, during time of measurement, is experienced due to the exposed nature of the antennas and the uncertainties in the drop size distribution throughout each rainfall, since rain rate is only measured at the link ends.

Buys and Janssen [20] compared the theoretical relationship between rain attenuation at 94 GHz and that of infrared with their relation obtained experimentally. They found that if the rain drop size is greater than about 0.6 mm, theoretical relations are in good agreement with the experimental data measured. This is not the case during drizzle.

Measurements at 94 GHz were made using a link 935 m long at the Hague, The Netherlands, whereas measurement at infra-red 3–5 μm were conducted with a transceiver located by the 94 GHz receiver, and a reflector 500 m apart. Three rain gauges, two located at both ends of the mm-link and one at the reflector, were used. Also employed was a distrometer at the receiver site.

Employing the same 94 GHz system, Keizer et al. [21, 22] obtained rain attenuation statistics. The measured rain attenuation, at vertical polarization and assuming uniform rainfall along the path, was compared with the calculated attenuation based on the actually measured drop size distributions as a function of rainfall rate.

Near Tokyo, Japan, Sasaki et al. [23] measured the rain attenuation at 20 GHz on 13 tandem links–considered to be approximately on a straight line–for about four years. The average path was 4.6 km and the total path was 60 km long. They examined quantitatively the spatial simultaneity of rain attenuation on each of these links. The overall rain probabilities of exceeding a given fade depth of any link

were expressed as the sum of the individual probabilities and were modified by the simultaneity of rain attenuation on each link. They developed a statistical analysis for the rain attenuation of the 13 tandem links.

Also in Japan, Hata and Doi [24] set up a 1.08 km mm-wave link, operating on 23 GHz and 40 GHz and situated in Nagoya city. They conducted a two year experiment and found that the measured path attenuation versus rain rate and the theoretical one based on Laws and Parsons distribution are in agreement, with some discrepancies at higher rain rate. They also analysed the statistics of heavy rain and found that it obeyed Poisson's distribution. They determined the best fit integration time to be 0.5 min for the 1.08 km–23 GHz link.

Norbury and White [25, 26] generated at the transmitter a vertically polarized signal (35.8 GHz). This signal was reflected from a corner-cube reflector to the receiving antenna placed adjacent to the transmitting antenna. The total path length was 448 m. They measured the excess path attenuation by compensating for an increase in pathloss by reducing the setting of a calibrated attenuator placed in the input waveguide of the receiver.

Sander [27] measured the attenuation coefficients as a function of rainfall rate, at the three wavelengths $\lambda = 5.77$, 3.3 and 2.0 mm. These coefficients were recorded at intervals of 60 sec. The average rainfall rates were measured along the 1 km propagation path for 60 sec intervals with three rain gauges. Three rain analysers were used to determine the drop size spectra, from which the 60 sec average rain rates were also computed. Attenuation coefficients were related to parameters that partially describe the drop size distribution of the rain. Also a comparison was made between the measured average drop size distribution with the distribution of Laws and Parsons.

All of the above experiments are summarized in Table 1. Many other experimental works have been carried out for investigating rain attenuation, on terrestrial or earth-space links, by direct methods or using radiometers.

A simple but useful empirical relation between rain attenuation A (dB) and rain rate R (mm/hr) based on radiometric measurements at 200 m height and at frequencies of 11, 18, and 22.2 GHz, and at different rainfall rates is: $A = (.094R)$ $f/11.0$ for 2.5 km path [28, 29], where f is the frequency in GHz. Values of A outside the above-mentioned frequencies can be satisfactorily obtained. The relation can be used for effective planning of communication links.

The rain intensity $R(x)$ is separated from parameters K and ε which depend on frequency f, raindrop size distribution and raindrop temperature in the following

Table 1. Rain Attenuation Measurements

Authors	Link Length	Freq. GHz.	Duration	Main Results
Ho *et al.* [18]	4.1 km	36–110	2 years	Rain attenuation at a given MMW frequency can be computed for a knowledge of the attenuation at another MMW frequency, and the use of LP distribution.
Weibel *et al.* [16]	2 km	90.5	1 year	A range of attenuation is measured against rainfall rate.
Buys *et al.* [21]	935 m	94	4 months	Theoretical relationship agrees well with experimental results for dropsize greater than 0.6 mm.
Keizer *et al.* [22]	935 m	94	8 months	Calculation of attenuation based on actually measured dropsize distribution as a function of rainfall rate.
Sasaki *et al.* [24]	13 links, 4.6 km each, approx.	20	4 years	A statistical analysis for rain attenuation over 13 tandem links.
Hata *et al.* [25]	1.08 km	23–40	2 years	Heavy rain statistics obeys Poisson's distribution—Best fit integration time is 0.5 for 1.08 km and 23 GHz
Norbury *et al.* [26]	448 m	35.8	1 year	Measurement of excess path attenuation.
Sander [27]	1 km	52, 90.8, 150	about 2 years	Measured attenuation coefficients are related to measured average dropsize distribution.

useful total attenuation A along the path of length L [30]:

$$A = K \int_0^L [R(x)]^{1+\varepsilon} \, dx, \quad \varepsilon < 0.3 \text{ for } f = 10 \text{ GHz to } 100 \text{ GHz}$$

For profile having same integral of rain intensity, namely 100 (mm/hr) km,

$$\alpha(x) = K[R(x)]^{1+\varepsilon} = 1.01 \times 10^{-2} [R(x)]^{1.27} \text{ at } 10 \text{ GHz}$$

$$\alpha(x) = 3.67 \times 10^{-2} [R(x)]^{1.15} \text{ at } 15 \text{ GHz}$$

In a spatially homogeneous rainfall over a short terrestrial propagation path of length L (km), the raindrop size distribution $N(D) = N_0 e^{-\alpha D}$ can be deduced

from measurements of rain attenuation A and rain rate R, using the following relation:

$$A = \gamma L = aRL, [31-33]$$

where

$$a = \gamma / R = \frac{\int_0^{D_{max}} 4.343 \times 10^3 Q(D)\, e^{-\alpha D}\, dD}{\int_0^{D_{max}} (6 \times 10^{-4} \pi v(D) D^3\, e^{-\alpha D}\, dD}$$

D, $v(D)$ and $Q(D)$ are the diameter, the fall velocity and the total extinction cross-section of a raindrop, respectively.

Attenuation due to Sand and Dust

Sand and dust storms usually contain particles with sizes ranging from a fraction of a micron to few hundred microns in radius. Due to the heavy particles of sand storms, which are never less than 0.04 mm in radius [34], the air two meters above the earth's surface could be clear of sand. Hence, we may expect that radio links will not be affected by sand storms, especially when antennas are mounted high enough.

Dust storms comprising much smaller particles (less than 0.1 mm in radius) may be found as high as hundred metres or more, and hence may affect the propagation in the millimeter waveband [35].

Sand and dust storms and the moisture content change the dielectric constant of the medium of propagation and, hence, its refractive index at millimeter wave frequencies. Therefore, considerable attenuation may be associated with such storms. A number of investigators have measured the refractive index of sand and dust [36–40]. However, few experimental systems, to the author's knowledge, were set up for measuring the effect of sand and dust. The experimental results of Al Hafid *et al.* [41] show much greater attenuation existed than predicted by theory. Theoretical calculations were very often used to predict the transmission parameters (attenuation) due to sand and dust [10, 35, 42], based on measured data for particles such as refractive index, particle shape and size.

The losses in the mm-wave propagation due to particulates, given in Sections 2.2, and 2.3, are summarized in Table 2.

It is interesting to note the following attenuation-constant α and phase-constant β relations [43], as effects of dust storms on microwave propagation, under actual conditions, namely, sand particles of different shapes (with correction factor C_s), and of probability density size distribution $\phi(r)$ and having vertical distribution

Table 2. Losses in MM Band

Fog	Clouds	Snow	Rain	Sand and Dust
Two orders of magnitude less than rain	Two orders of magnitude less than rain	Less than rain of the same water content	Dominant and can reach 30 dB/km	Scattering and absorption reach 2-3 dB/km
Increases as the frequency increases or visibility decreases	Increases as frequency increases	For wet snow and melting hailstones or sleet losses can reach 4 dB under strong snowfall condition	Increases with rain rate or with frequency	Significant at higher frequency band (above 10 GHz)
	Clouds effect appears mainly in earth-space communication			
	Losses are present for much of the time in many climates	Ice and dry snow exhibit very low loss		Increases as visibility decreases. Visibility can reach several metres.

$N(Z)$ of particle concentration:

$$\alpha = \frac{1.029 \times 10^6 \varepsilon''}{[(\varepsilon'+2)^2 + \varepsilon''^2]\lambda} C_s N(Z) \int_0^{r_{max}} \phi(r)r^3 \, dr \text{ db/km}$$

$$\beta = \frac{2.26 \times 10^6 (\varepsilon^2 + \varepsilon''^2 + \varepsilon' - 2)}{[(\varepsilon'+2)^2 + \varepsilon''^2]\lambda} C_s N(Z) \int_0^{r_{max}} \phi(r)r^3 \, dr \text{ Degree/km}$$

where ε', ε'' are the real and imaginary parts of the dielectric constant of dust material, λ is the operation wavelength (metres), r is the particle radius.

Scintillation

Signal scintillations are small random fluctuations in the phase and amplitude of the received signal caused by the turbulent fluctuations of refractive index of the troposphere. This turbulence has an outer scale as well as an inner scale. Millimetric wave fluctuations are mainly dependent on atmospheric refractive index fluctuations, the wavelength of the radio signal, the propagation path length and the size of the outer scale of turbulence.

Weibel et al. [16] found that strong scintillations (above 1.5 dB) occurred during days of wind gusts, while weak scintillations (below 1.5 dB) occurred during clear

days (humidity below 50% and wind velocity below 10 mph). Clifford and Strohbehn [44] showed that in deriving the spectra for the phase and amplitude fluctuations, for a microwave signal propagated over a line of sight path through a turbulent medium, the results derived under the assumption $\lambda \ll l_0$ are equally valid for $\lambda > l_0$, where l_0 is the inner scale of turbulence. These results were derived directly from the wave equation. Lane [45] concluded that amplitude scintillations of up to 10 dB may be expected on terrestrial links in the frequency range 35–100 GHz. For earth-space links the maximum values does not exceed 4 dB.

Measurements of signal fluctuations (in both amplitude and phase) were made by several authors and under different weather conditions. Table 3 summarizes some of these experiments.

Table 3.   Amplitude and Phase Scintillations Measurements

Author	Freq. GHz	Atmospheric Condition	Main Results
Ho *et al.* [46–48]	36–110	Town environment–no precipitation on a summer day	Maximum value of A.S. occurs around noon, and minimum around midnight.
			Log normal distributions of A.S. at 36 and 110 GHz
		Town environment– output of an air conditioning plant near the link path	Log amplitude of fluctuations is the sum of the log amplitude fluctuations due to variations of refractive index caused by atmospheric turbulence and those caused by the output of the air conditioning plant.
Vilar and Matthews [49]	36.1	Town environment– normal	A.S. can be up to ten times greater during the day than at night. Both phase and refractive index spectra have similar slope in the log-log scale
Millman [50]	15.3	Clear	A.S. less than 1.5 dB with periods of less than 1 minute. r.m.s. phase fluctuations decrease linearly with frequency.
		Passage of a cold front	A.S. could reach 5 dB.
		Strong ground moisture	Long term fades up to 6 dB.
Etcheverry *et al.* [51]	94	Non-turbulent– clear–calm	A.S. not exceeding 1 dB peak to peak. Small phase differences for 1 m antenna separation.
		Clear, 2–5 knot wind	A.S. larger and more rapid, 3 dB peak to peak. 90° phase difference for 7 m antenna separation.
		During diesel, fuel, oil and rubber burn	A.S. about 3 dB peak to peak

A.S. stands for Amplitude Scintillation.

Outline of Part 2

In the second part of this paper; multipath fading and depolarization are treated. Experimental work on diversity improvement, together with a brief on data processing is also given. Some areas of needed measurements are outlined and the conclusion of the two parts is presented as well.

References

Review Papers

1. **Pratt, T.,** A review of some cross-polarization effect on slant paths in the 11–30 GHz frequency range, *AGARD Conf. Proc.* No. 284, pp. 11-1 to 11-9 (Aug. 1980).

2. **Stephansen, E.T.,** Clear-air propagation on line-of-sight radio path: a review, *Radio Science*, **16**, No. 5, pp. 609–629 (Sept.–Oct. 1981).

3. **Olsen, R.L.,** Cross polarization during precipitation on terrestrial links: a review, *Radio Sci.*, **16**, No. 5, pp. 761–779 (Sept.–Oct. 1981).

4. **Olsen, R.L.,** Cross polarization during clear-air conditions on terrestrial links: a review, *Radio Sci.*, **16**, No. 5, pp. 631–647 (Sept.–Oct. 1981).

5. **Watson, P.A.,** Survey of measurements of attenuation by rain and other hydrometers, *Proc. IEE*, **123**, No. 9, pp. 863–871 (1976).

6. **Davis, P.G.** and **Mackenzie, E.C.,** Review of SHF and EHF slant path propagation measurements made near Slough (UK), *IEE Proceedings*, **128**, Pt. H, No. 1, pp. 53–65 (1981).

7. **Crane, R.K.,** Attenuation due to rain—a mini-review, *IEEE Transactions on Antennas and Propagation*, **AP-23**, pp. 750–752 (1975).

8. **Vonder Vorst, A.S.,** A survey of atmospheric propagation research experiment on slant paths, in the band 15–40 GHz, *Agard Conf. Pub.*, No. 254, pp. 41-1/41-17 (1978).

9. **Fischer, K.,** Amt fur Wehrgeophysik, *Agard Conf. Proc.*, No. 245, Millimeter & Submillimeter Wave Propagation & Circuits, pp. 42-1/42-5 (1978).

10. **Goldhirsh, J.,** A parameter review and assessment of attenuation and backscatter properties associated with dust storms over desert regions in the frequency range of 1 to 10 GHz, *IEEE Trans. on Antennas and Propagation*, **AP-30**, No. 6, pp. 1122–1127 (Nov. 1982).

Free Space Attenuation

11. **Flood, W.A.,** Overview of near millimeter wave propagation, *SPIE*, **259**, pp. 52–57 (1980).

12. **Burton, J.M.** and **Vinnal, E.,** Radio propagation above 10 GHz, Part 1: An overview of new frequency band, *Telecommunications Journal of Australia*, **30**, No. 3, pp. 210–215 (1980).

13. **Liebe, H.J.,** *et al.*, Atmospheric oxygen microwave spectrum—experiment versus theory, *IEEE Trans. on Ant. and Prop.*, **AP-25**, No. 3 (1977).

14. **Saveskie, P.N.,** *Radio Propagation Handbook*, Tab-Books Inc. (1980).

Attenuation due to Hydrometeors

15.   **Hogg, D.C.** and **Chu, T.**, The role of rain in satellite communications, *Proc. IEEE*, **63**, No. 9, pp. 1308-1331 (Sept. 1975).

16.   **Weible, G.E.** and **Dressel, H.O.**, Propagation studies in millimeter wave link systems, *Proc. IEEE*, **55**, No. 4, pp. 497-512 (1967).

17.   **Ryde, J.W.** and **Ryde, D.**, Attenuation of centimeter and millimeter waves by rain, hail, fogs and clouds, *Rep. 8670*, GE CO. Research Lab., Wembley (May 1945).

18.   **Ho, K.L., Mavrokoukoulakis, N.D.** and **Cole, R.S.**, Propagation studies on a line-of-sight microwave link at 36 GHz and 110 Ghz, *Microwaves, Optics and Acoustics*, **3**, No. 3, pp. 93-97 (1979).

19.   **Turner, D., Easterbrook, B.J.** and **Golding, J.E.**, Experimental investigation into radio propagation at 11.0-11.5 GHz, *IEEE Proc.*, **113**, No. 9, pp. 1477-1489 (Sept. 1966).

20.   **Buys, J.H.** and **Janssen, L.H.**, Comparison of simultaneous atmospheric attenuation measurement at visible light, mid-infrared (3-5 μm) and millimeter waves (94 GHz), *IEE Proc.*, **128**, Pt. H, No. 3, pp. 131-136 (1981).

21.   **Keizer, W.P.M.N., Snieder, J.** and **deHaan, C.D.**, Rain attenuation measurement at 94 GHz; comparison of theory and experiment, *AGARD Conf. Proc.*, No. 254, pp. 44-1/44-9 (1978).

22.   **Keizer, W.P.M.N., Snieder, J.** and **deHaan, C.D.**, Propagation measurements at 94 GHz and comparison of experimental rain attenuation with theoretical results derived from actually measured raindrop size distribution, *Intl. Conf. on Antennas and Propagation, IEE Conf. Pub.*, **169**, pp. 72-76 (1978).

23.   **Sasaki, O., Nagamune, I., Sato, K.** and **Hosoya, Y.**, Rain attenuation characteristics on 20 GHz band multirelay links, *IEEE Trans. on Antennas and Propagation*, **AP-29**, No. 4, pp. 587-594 (1981).

24.   **Hata, M.** and **Doi, S.**, Propagation tests for 23 GHz and 40 GHz, *IEEE Journal on selected areas in communications*, **SAC-1**, No. 4, pp. 658-673 (Sept. 1983).

25.   **Norbury, J.R.** and **White, W.J.K.**, Microwave attenuation at 35.8 GHz due to rainfall, *Electronic Letters*, **8**, No. 4, pp. 91-92 (1972).

26.   **Norbury, J.R.** and **White, W.J.K.**, Correlation between measurements of rainfall rate and microwave attenuation at 36 GHz, *IEE Conf. Pub.*, **98**, pp. 45-51 (1973).

27.   **Sander, J.**, Rain attenuation of millimeter waves at λ = 5.77, 3.3, and 2 mm, *IEEE Trans. on Antenna and Propagation*, **AP-23**, No. 2, pp. 213-230 (1975).

28.   **Atshuler, E.E.**, A simple expression for estimating attenuation by fog at millimeter wavelengths, *IEEE Trans. on Antennas and Propagation*, **AP-32**, pp. 757-758 (July 1984).

29.   **Raina, M.K.** and **Upal, G.S.**, Frequency dependence of rain attenuation measurements at microwave frequencies, *IEEE Trans. on Antennas and Propagation*, **AP-32**, pp. 185-187 (Feb. 1984).

30.   **Paraboni, A.**, Characterization of rain profiles in a second-order approximation and application to attenuation beyond 10 GHz, *IEEE Trans. on Antennas and Propagation*, **AP-30**, pp. 396-400 (May 1982).

31.   **Manabe, T., Ihara, T.** and **Funihama, T.**, Inference of raindrop size distribution from attenuation and rain rate measurements, *IEEE Trans. on Antennas and Propagation*, **AP-32**, pp. 474-478 (May 1984).

32. **House, R. Jr.,** Structures of atmospheric precipitation systems; a global survey, *Radio Science,* **16,** No. 5, p. 671 (Sept. 1981).

33. **Hathaway, S.D.** and **Evans, H.W.,** Radio attenuation at 11 kmc and some implications affecting relay system engineering, *BSTJ,* **38,** p. 73 (Jan. 1959).

Attenuation due to Sand and Dust

34. **Bagnold, R.A.,** *The Physics of Blown Sand and Desert Dunes,* Chapman & Hall, UK (1973).

35. **Ansari, A.J.** and **Evans, B.G.,** Microwave propagation in sand and dust storms, *IEE Proc.,* **129,** Pt. F, No. 5 (1982).

36. **Ahmed, L.Y.** and **Auchterlonie, L.J.,** Microwave measurements on dust at x-band, *Electron Lett.,* **16,** No. 10 (May 1980).

37. **Ghobrial, S.I.,** The effect of sand storms on microwave propagation, *Proc. Nat. Telecommun. Conf., Houston, TX.,* **2,** Proc. No. CH1539-6/80/0000-0216, pp. 43.5.1, 43.5.4 (1980).

38. **Ghobrial, S.I.,** Effect of hydroscopic water on dielectric constant of dust at x-band, *Elect. Letter,* **16,** No. 10 (May 1980).

39. **Thompson, J.H.,** Dust cloud modeling and propagation effects for radar and communication codes, *Technical Report NA46977,* 93102, Santa Barbara, CA. (1980).

40. **Stuchly, S.S.,** Dielectric properties of some granular solids containing water, *J. Microwave Power,* **5,** No. 2, pp. 62-68 (1970).

41. **Al-Hafid, H.T., Gupta, S.C., Al-Mashadani, M.** and **Buni, K.,** Study of microwave propagation under adverse dust storm conditions, *Third World Telecommunications forum, Geneva* (1979).

42. **Bashir, S.O., Dissanayake, A.W.** and **McEwan, N.I.,** Prediction of forward scattering and cross-polarization due to dry and moist haboub and sand storms in Sudan in the 9.4 GHz band, *Telecommunication J.,* **47-VII,** pp. 462-467 (1980).

43. **Salem, I., Sakr, D.L.** and **Maghraby, S.,** More realistic analysis of the effect of dust storms on M.W. propagation, *National URSI Symposium* (1983).

Scintillation

44. **Clifford, S.F.** and **Stohbehn, J.W.,** Theory of microwave line-of-sight propagation through a turbulent atmosphere, *IEEE Trans. on Antennas and Propagation,* **AP-18,** pp. 264-274 (March 1970).

45. **Lane, J.A.,** Scintillation and absorption fading on line-of-sight links at 35 and 100 GHz, *Proc. IEE,* **48,** pp. 166-174 (1968).

46. **Ho, K.L., Cole, R.S.** and **Mavrokoukoulakis, N.D.,** Spectral analysis of anomalous millimeter wave amplitude scintillation in a town environment, *IEEE Trans. on Antennas and Propagation,* **AP-28,** No. 6, pp. 941-942 (1980).

47. **Ho, K.L., Mavrokoukoulakis, N.D.** and **Cole, R.S.,** Determination of the atmospheric refractive index structure parameter from refractivity measurement and amplitude scintillation measurement at 36 GHz, *Journal of Atmospheric and Terrestrial Physics,* **40,** pp. 745-747 (1978).

48. Ho, K.L., Mavrokoukoulakis, N.D. and Cole, R.S., Wavelength dependence of scintillation fading at 100 and 36 GHz, *Electronics Letters*, 13, No. 7, pp. 181–183 (1977).

49. Vilar, E.M. and Matthews, P.A., Summary of scintillation observation in a 36 GHz link across London, *IEE Conf. Pub.*, 169, Pt. 2, pp. 36–40 (1978).

50. Millman, G.H., Tropospheric effects on space communications, *AGARD-CP-70*, Dusseldorf, pp. 4.1 to 4.29 (1970).

51. Etcheverry, R.D., Heidlreder, G.R., Johnson, W.A. and Weitraub, H.I., Measurements of spacial coherence in 3.2 mm horizontal transmission, *Trans. IEEE*, AP-15, pp. 136–141 (1967).

استعراض للدراسات الميدانية عن وصلات الراديو المليمترية الأرضية
الجزء الأول : الاضمحلال بسبب الأجزاء العالقة في الجو

عادل علي ، محمد حسن و محمد الحيدر
قسم الهندسة الكهربائية ـ جامعة الملك سعود ـ
الرياض ـ المملكة العربية السعودية

تستعرض هذه الورقة الدراسات الميدانية على وصلات الراديو المليمترية الأرضية .
في الجزء الأول سنقوم باستعراض الاضمحلال نتيجة وجود العوامل الجوية
المختلفة كالضباب ، والسحب والثلج والمطر كما سنقوم بالتركيز على تأثير المطر .
أما فيما يتعلق بالعواصف الرملية والغبار فهناك دراسة أخرى ولا يتسع المجال
لذكرها هنا .

وتبدأ الدراسة بايضاح الظواهر الطبيعية يلي ذلك تلخيص لأحدث التجارب
مع التأكيد على نوعية الأجهزة المستخدمة وأهم النتائج . وفي الجزء الثاني سنقوم
بمناقشة الظواهر المتعلقة بالانتشار في الأجواء الصافية وكذلك التنوع ومعالجة
المعلومات أما فيما يتعلق بالتمثيل والدراسات النظرية والمسارات المائلة فإنها تقع
خارج نطاق الدراسة .